



Published in final edited form as:

Cell Rep. 2014 September 11; 8(5): 1461–1474. doi:10.1016/j.celrep.2014.07.053.

Hexokinase 2-Mediated Warburg Effect Is Required for *PTEN* and *p53*-Deficiency Driven Prostate Cancer Growth

Lei Wang^{1,6}, Hua Xiong^{1,6}, Fengxia Wu^{1,6}, Yingjie Zhang¹, Ji Wang¹, Liyan Zhao¹, Xiaolan Guo¹, Li-Ju Chang¹, Yong Zhang², M. James You³, Shahriar Koochekpour⁴, Mohammad Saleem¹, Haojie Huang⁵, Junxuan Lu², and Yibin Deng^{1,*}

¹The University of Minnesota Hormel Institute, Austin, MN, 55912, USA

²Department of Biomedical Sciences, Texas Tech University Health Sciences Center School of Pharmacy, Amarillo, TX, 79106, USA

³Department of Hematopathology, The University of Texas M.D. Anderson Cancer Center, Houston, TX, 77030, USA

⁴Department of Cancer Genetics, Center for Genetics and Pharmacology Roswell Park Cancer Institute, Buffalo, NY, 14263, USA

⁵Department of Biochemistry and Molecular Biology, Mayo Clinic College of Medicine, Rochester, MN, 55905, USA

Summary

Accumulating evidence suggests that co-deletion of tumor suppressor genes *Pten* and *p53* plays a crucial role in the development of castration-resistant prostate cancer *in vivo*. However, the molecular mechanism underlying *Pten/p53*-deficiency driven prostate tumorigenesis remains incompletely understood. Building upon insights gained from our studies with *Pten/p53*-deficient mouse embryonic fibroblasts (MEFs), we report here that hexokinase 2 (HK2) is selectively upregulated by the combined loss of *Pten* and *p53* in prostate cancer cells. Mechanistically, *Pten* deletion increases HK2 mRNA translation through activation of the AKT-mTORC1-4EBP1 axis

© 2014 The Authors. Published by Elsevier Inc. All rights reserved.

*Correspondence author: Yibin Deng, M.D., Ph.D., The University of Minnesota Hormel Institute, 801 16th Ave NE, Austin, MN 55912, USA, Tel: 507-437-9611; Fax: 507-437-9606, yideng@hi.umn.edu.

⁶These authors contributed equally to this work

Supplemental Information

Supplemental information includes Supplementary Experimental Procedures, Seven Supplementary Figures with Figure Legends, and Supplementary References.

Author Contributions

L. W. performed animal studies, hematoxylin and eosin staining, and immunohistochemistry on prostate cancer samples. H.X. and F.W. performed cell culture and tumor xenograft studies. Y.Z., J. W., L.Z., X.G., L.C., Y. Z., and S. M. helped with the cell culture and animal experiments and generated data. M.J. Y. provided *Pten* conditional knockout mice and technical support. S.K. provided human prostate tumor samples for TMA. H.H. and J.L. provided conceptual advice, assisted with the design of animal experiments, and helped to edit the manuscript. Y.D. conceived this study, designed the experiments, analyzed and interpreted the data, and wrote the manuscript.

Publisher's Disclaimer: This is a PDF file of an unedited manuscript that has been accepted for publication. As a service to our customers we are providing this early version of the manuscript. The manuscript will undergo copyediting, typesetting, and review of the resulting proof before it is published in its final citable form. Please note that during the production process errors may be discovered which could affect the content, and all legal disclaimers that apply to the journal pertain.

and *p53* loss enhances HK2 mRNA stability through inhibition of miR143 biogenesis. Genetic studies demonstrate that HK2-mediated aerobic glycolysis, known as the Warburg effect, is required for *Pten/p53*-deficiency driven tumor growth in xenograft mouse models of prostate cancer. Our findings suggest that HK2 might be a therapeutic target for prostate cancer patients carrying *Pten* and *p53* mutations.

INTRODUCTION

Prostate cancer is the second leading cause of cancer-related deaths in men after lung cancer in the USA. Prostate cancer arises mainly from prostatic intraepithelial neoplasia (PIN), a precursor lesion that ultimately progresses to adenocarcinoma and metastatic diseases (DeMarzo et al., 2003). The initiation, progression, and metastasis of prostate cancer involve alterations of multiple tumor suppressor genes, such as *Pten* (phosphatase and tensin homolog deleted on chromosome 10) and *p53* (Shen and Abate-Shen, 2010). Loss of one allele of *Pten* occurs frequently in primary prostate cancers, and homozygous deletion of *Pten* is found in 70% of advanced prostate cancers (Cairns et al., 1997; Gray et al., 1995; Suzuki et al., 1998; Whang et al., 1998). Similarly, *p53* is often found completely lost or mutated in advanced human prostate cancers (Navone et al., 1999). Recent advances in whole-genome/exome-sequencing analyses reveal that *Pten* and *p53* are often co-deleted or co-mutated in lethal castration-resistant prostate cancers (CRPC) (Grasso et al., 2012). Systems bioinformatics analyses estimate that prostate cancers with combined loss of *Pten* and *p53* make up 11% of highly aggressive prostate cancers and bestow the worst survival outcome for patients (Markert et al., 2011). Importantly, tracking the clonal origin of lethal prostate cancer through patient samples collected during tumor progression and at the time of death identified that the lethal metastatic clone arose from primary prostate cancer cells carrying *Pten* deletion and mutant *p53* (Haffner et al., 2013). Mouse genetic studies suggest that *Pten* deletion in prostate epithelial cells primarily initiates PIN, whereas *p53* loss in prostate epithelial cells is not sufficient to cause any distinguishable morphological phenotypes *in vivo*. However, double deletion of *Pten* and *p53* in prostate epithelial cells leads to invasive prostate cancer with salient features of human CRPC (Lunardi et al., 2013; Deng et al., unpublished data). These clinical and experimental findings implicate that loss of *Pten* and *p53* in prostate epithelial cells plays a causal role in CRPC. However, the molecular mechanism underlying *Pten* and *p53*-deficiency driven prostate tumorigenesis remains incompletely understood.

PTEN, by dephosphorylating the 3' position of phosphatidylinositol-3,4,5-trisphosphate (PIP3) to phosphatidylinositol 4,5-bisphosphate (PIP2), antagonizes the phosphatidylinositol-3-OH kinase (PI3K)-AKT signaling pathway that stimulates cell metabolism, growth, and survival (Song et al., 2012). Downstream of the PI3K-AKT kinase pathway, mammalian target of rapamycin (mTOR) assembles with regulatory-associated protein of mTOR (Raptor) to form mTOR Complex 1 (mTORC1) or with Rictor to form mTOR Complex 2 (mTORC2) (Guertin and Sabatini, 2007). Both complexes exert their actions by phosphorylating their unique substrates. mTORC1 phosphorylates p70 ribosomal protein S6 kinase (S6K) and 4E-binding protein 1 (4E-BP1; also known as eIF4E-BP1) to increase protein synthesis, which facilitates cell survival, proliferation and growth (Laplanche

and Sabatini, 2012). mTORC2 facilitates the activation of AKT by phosphorylating AKT on serine 473 (Jacinto et al., 2006; Sarbassov et al., 2005). Studies of genetically-engineered prostate cancer mouse models coupled with whole-genome/exome sequencing analyses of human prostate cancers suggest that aberrant activation of the PI3K-AKT-mTOR signaling pathway plays a causal role in *Pten*-deficiency driven prostate tumorigenesis (Barbieri et al., 2012; Chen et al., 2006; Grasso et al., 2012). Interestingly, it has been shown recently that loss of *Pten* induces ER UDPase ectonucleoside triphosphate diphosphohydrolase 5 (ENTPD5), and activation of the AKT/mTOR pathway leads to induction of pyruvate kinase isoenzyme type M2 (PKM2), which contribute to aerobic glycolysis, also known as the Warburg effect, and tumor growth in a xenograft model of prostate cancer (Fang et al., 2010; Sun et al., 2011). These results suggest that dysregulation of the PTEN-PI3K-AKT-mTOR pathway in prostate cancer cells could cause the Warburg effect, which in turn facilitates prostate cancer development.

The well-established tumor suppressor protein p53 plays important roles not only in mediating cell cycle arrest, senescence, autophagy, and apoptosis, but also in regulating cell metabolism. p53 inhibits aerobic glycolysis by inducing expression of the TP53-induced glycolysis and apoptosis regulator (TIGAR) (Bensaad et al., 2006) and Parkin (Zhang et al., 2011), or by decreasing the expression of glycolytic enzyme phosphoglycerate mutase 1 (PGAM1) (Kondoh et al., 2005). p53 shifts cellular metabolism and energetics from the glycolytic pathway toward the respiratory pathway through induction of synthesis of cytochrome C oxidase 2 (SCO2) (Matoba et al., 2006). p53 also enhances mitochondrial respiration by inducing glutaminase 2 (GLS2) (Hu et al., 2010; Suzuki et al., 2010). In addition, p53 can directly interact with glucose-6-phosphate dehydrogenase (G6PD) to suppress the pentose phosphate pathway (PPP), which branches out from glycolysis by utilizing glycolytic intermediates to produce metabolites vital for biosynthesis (Jiang et al., 2011). Therefore, the loss or mutation of p53 might promote and sustain tumor growth by enhancing the Warburg effect and anabolic (biosynthesis) pathways.

Hexokinases (HKs) catalyze the essentially irreversible first step of glycolytic pathway by phosphorylating glucose to glucose-6-phosphate (G-6-P). There are four isoforms encoded by the separate genes: HK1, HK2, HK3, and HK4 (also known as glucokinase). HK1 is ubiquitously expressed in almost all mammalian tissues, and HK2 is normally expressed in insulin-sensitive tissues such as adipose, skeletal, and cardiac muscles. HK3 is usually expressed at low levels and HK4 expression is restricted to the pancreas and liver (Wilson, 2003). High level of HK2 expression has been observed in cancer cells and is associated with poor overall survival in cancer patients (Mathupala et al., 2001; Wolf et al., 2011). Importantly, genetic studies utilizing mouse models demonstrated that HK2 plays an essential role in *Kras*-driven lung cancer and *ErbB2*-driven breast cancer *in vivo* (Patra et al., 2013). However, whether and how loss of *Pten* and *p53* in prostate epithelial cells induces HK2-mediated Warburg effect to contribute to prostate tumorigenesis has not yet been explored.

Through integrated analyses of *Pten/p53*-deficient mouse embryonic fibroblasts (MEFs), prostate cancer cell lines, xenografts, and genetically engineered mouse models as well as clinic prostate cancer samples, we show herein that *Pten/p53*-deficiency selectively

enhances expression of HK2, but not HK1, through posttranscriptional and translational regulation. More importantly, genetic studies suggest that HK2-mediated Warburg effect is required for *Pten* and *p53*-deficiency driven prostate tumor growth *in vivo*.

RESULTS

HK2-Mediated Warburg Effect Is Required for Cell Transformation and Tumorigenesis

To study whether and how loss of *Pten* and *p53* causes tumorigenesis, we generated primary mouse embryonic fibroblasts (MEFs) carrying either floxed *Pten* alleles (*Pten*^{F/F}*p53*^{+/+}), floxed *p53* alleles (*Pten*^{+/+}*p53*^{F/F}) or both (*Pten*^{F/F}*p53*^{F/F}) (Figures S1A and S1B). Subsequent Cre-loxP-mediated recombination gave rise to cells deficient in either *Pten* (*Pten*^{-/-}*p53*^{+/+}), *p53* (*Pten*^{+/+}*p53*^{-/-}) or both (*Pten*^{-/-}*p53*^{-/-}), as evident by PCR genotyping and Western blot analysis (Figures S1C and S1D). We confirmed that loss of *Pten* activated p53-mediated senescence as reported previously (Chen et al., 2005), whereas loss of *p53* caused immortalization of MEFs as the cells bypassed senescence (Figures S2A–S2C). While neither single deletion of *Pten* nor *p53* in MEFs led to cellular transformation, double deletions of *Pten* and *p53* transformed MEFs and endowed them with the ability to form tumor in NOD/SCID IL2RG (NSG) mice (Figures S2D–2G). Our findings suggest that the combined inactivation of *Pten* and *p53* in MEFs is sufficient and required to cause cell transformation and tumorigenesis *in vivo*.

As the culture media of *Pten*^{-/-}*p53*^{-/-} MEFs turned yellow much faster than that of *Pten*^{+/+}*p53*^{-/-} MEFs, we hypothesized that this phenotype might be due to lactate acidosis. Indeed, glucose consumption and lactate production were significantly increased in *Pten*^{-/-}*p53*^{-/-} MEFs compared with *Pten*^{+/+}*p53*^{-/-} MEFs (Figures 1A and 1B). Since these metabolic changes resembled aerobic glycolysis, we screened for the molecular candidates contributing to the alterations of glucose and lactate metabolism by immunoblotting. HK2, but not HK1, was identified to be markedly elevated in *Pten/p53*-deficient MEFs (Figure 1C).

We then knocked down HK2 expression in *Pten/p53*-deficient MEFs to investigate whether it was required for induction of the Warburg effect and tumor formation *in vivo*. Lentivirus-mediated shRNA targeting mouse HK2 caused a significant reduction of endogenous HK2 but not HK1 (Figure 1D). Depletion of HK2 in *Pten/p53*-deficient MEFs significantly reduced glucose consumption (Figure 1E) and lactate production (Figure 1F), attenuated anchorage-independent cell growth on soft agar (Figures 1G and 1H), and impaired tumor growth in a xenograft model (Figure 1I). Note the HK2 depletion-caused phenotypes were observed in the presence of a physiological level of HK1. However, exogenous expression of the human HK2, which is resistant to silencing by the shRNA targeting mouse HK2, rescued the phenotypes observed in mouse HK2-depleted MEFs (Figures 1E–1I). These results support that HK2-mediated Warburg effect is required for *Pten/p53*-deficiency-induced MEFs transformation and tumorigenesis *in vivo*.

Loss of *Pten* and *p53* in Prostate Epithelial Cells Robustly Enhances HK2 Protein Expression

To determine whether the increased HK2 expression in *Pten/p53*-deficient MEFs could be observed in human prostate cancer cells carrying similar genetic aberrations, we screened several human prostate cancer cell lines for HK2 protein expression by immunoblotting. As shown in Figure 2A, HK2 was significantly elevated in PC3 cells (*Pten/p53*-deficiency) compared with LNCaP cells (*Pten*-deficiency with wild-type *p53*), but no signal or very weak HK2 expression was detected in DU145 cells (wild-type *Pten* with mutant *p53*) or the non-tumorigenic human prostate epithelium RWPE-1 cells (wild-type *Pten* with functionally inactivated *p53*). To pathogenetically simulate the *Pten* change as in PC3 cells, we established DU145 and RWPE-1 cells stably expressing two different sets of shRNA for human *Pten*. Depletion of *Pten* in DU145 and RWPE-1 cells induced HK2 expression (Figures 2B and 2E), accompanied by increased glucose consumption (Figures 2C and S3A) and lactate production (Figures 2D and S3B) in the respective cell line. Importantly, reduction of *Pten* promoted the transformation of RWPE-1 cells, as evident by their acquired ability to grow in soft-agar (Figures S3C and S3D). However, there was no significant difference of HK1 protein expression in these cells upon *Pten* depletion (Figures 2B and 2E). These data suggest that inactivation of *Pten* in human prostate epithelial cells with mutant or inactivated *p53* is sufficient for the enhanced expression of HK2 without affecting HK1, and that HK2 in turn facilitates the Warburg effect and drives cell transformation.

To determine whether HK2 expression in prostate epithelial cells is increased upon loss of *Pten* and *p53* *in vivo*, we collected prostate tissue from genetically engineered mouse models with deletion of either *Pten* or *p53* and deletion of both specifically in prostate epithelial cells by crossbreeding mice harboring *Probasin-Cre4* (*Pb-Cre4*) (Wu et al., 2001), floxed *Pten* alleles (Zheng et al., 2008) and/or floxed *p53* alleles (Jonkers et al., 2001). Genetic deletions were confirmed by PCR genotyping (Figure S4A), IHC staining (Figure S4B), and Western blot (Figure 2G). By 20 weeks of age, the prostate tumor in *Pten/p53*-deficient mice encompassed the entire genitourinary tract. In contrast, *Pten*-deficient mice retained recognizable but enlarged anterior prostate (AP), ventral prostate (VP) and dorsolateral prostate (DLP) lobes (Figure S5A). The average tumor weight in *Pten/p53*-deficient mice was 20 times that of *Pten*-deficient mice (Figure S5B). Histopathology of *Pten/p53*-deficient prostate tumors indicated invasive carcinomas, whereas *Pten*-deficient prostate had mainly high-grade prostatic intraepithelial neoplasia (HG-PIN). However, prostate histology of age-matched *p53*-deficient mice did not differ from those of the wild-type mice (Figure 2F).

As expected (Chen et al., 2005), *Pten* deletion in prostate epithelial cells resulted in AKT phosphorylation and p53 induction (Figure 2G, lane 3 vs. 1). Whereas HK2 protein expression was below the limit of detection in wild type (WT) or *p53*-deficient prostate (Figure 2G, lanes 1 and 4), it was detectable in *Pten*-deficient prostate (Figure 2G, lane 3) and was significantly enhanced in *Pten/p53*-deficient prostate analyzed by Western Blot (Figure 2G, lane 2) and confirmed by IHC staining (Figures 2H and 2I). However, no significant changes of HK1 protein expression were observed in the prostate with various

genotypes (Figure 2G). These findings support that co-deletions of *Pten* and *p53* in prostate epithelial cells selectively enhance HK2 expression in mouse models.

PTEN Deletion Increases HK2 mRNA Translation through AKT-mTORC1-4EBP1 Signaling

To understand the molecular mechanism underlying how loss of *Pten* and/or *p53* upregulates HK2, we examined HK2 mRNA level in MEFs with defined genetic changes by real time RT-PCR. HK2 mRNA expression was not induced upon loss of *Pten* (Figure 3A, column 2 vs. 1), whereas it was dramatically increased in MEFs with loss of *p53* (Figure 3A, column 3 vs. 1). No further enhanced HK2 mRNA was observed in *Pten/p53*-deficient MEFs (Figure 3A, column 4 vs. 3). To exclude cell type-dependent regulatory mechanisms, we analyzed HK2 mRNA expression in prostate tissue/tumors derived from *Pten* and/or *p53* conditional knockout mouse models and observed identical results as in MEFs (Figure 3C). It is particularly noteworthy that *p53* deletion increased HK2 mRNA (Figures 3A and 3C) but failed to increase the HK2 protein level (Figure 2G), whereas *Pten* deletion did not increase HK2 mRNA (Figures 3A and 3C) yet increased HK2 protein, although not to the significant extent as the double deletion of *Pten* and *p53* achieved (Figure 2G). We also examined HK2 mRNA levels in *Pten*-depleted-DU145 or -RWPE-1 cell and found no difference with their respective parental cells (Figures S6A and S6B). Interestingly, HK2 mRNA expression in DU145 cells is significantly elevated compared to LNCaP cells (Figure S6C). However, expression of protein HK2 in DU145 cells is barely detected (Figure 2A). No significant difference of HK1 mRNA was observed in these models carrying various genotypes (Figures 3B, 3D and S6D). These data together suggest the possibility that *p53* selectively regulates HK2 at the mRNA level, whereas *Pten* predominantly regulates HK2 at the protein level.

Given that previous studies supported that AKT-mTORC1 pathway plays an important role in *Pten*-deficiency driven prostate tumorigenesis, we utilized both genetic and pharmacological approaches to determine the role of AKT-mTORC1-4EBP1-mediated 5' cap-dependent translation signaling in upregulating HK2 protein expression upon *Pten* deletion. Depletion of AKT or Raptor (an essential component of mTORC1 complex) by shRNAs in *Pten/p53* double-deficient MEFs reduced HK2 protein expression but had no effect on HK1 protein expression (Figures 3E and 3F). Knockdown of AKT or Raptor in prostate cancer cell line (UMN-4240P), derived from a prostate tumor in *Pten/p53*-deficient mouse (Figures 3I and 3J) or in human prostate cancer cell line (PC3) (Figures 3M and 3N), resulted in a significant reduction of protein expression of HK2, but little if any effect on HK1 expression (Figures 3I, 3J, 3M, and 3N). Furthermore, pharmacological inhibition of the AKT-mTORC1-mediated translation pathway in PC3 cells with the PI3K-mTOR dual inhibitor NVP-BEZ235 remarkably reduced protein expression of HK2, but not HK1 (Figure 4E). In contrast to a marked reduction of HK2 protein expression, there was no significant decrease of HK2 mRNA in the AKT- or Raptor-depleted multiple cell lines or BEZ235-treated PC3 cells (Figures 3G, 3H, 3K, 3L, 3O, 3P, and S6E), suggesting AKT-mTORC1 signaling primarily regulates HK2 expression at the translational level. In support of this possibility, loss of *Pten* increased the amount of HK2 mRNA loaded on the polysome (Figures 4A and 4B), whereas genetic inhibition of AKT-mTORC1 signaling significantly

decreased polysome-associated HK2 mRNA (Figures 4C and 4D), while the amount of total HK2 mRNA remained unaffected (Figures 4B–4D).

The allosteric mTOR inhibitor rapamycin had minimal effects on HK2 protein levels compared with BEZ235 (Figure 4E). BEZ235 significantly inhibited activation of two primary downstream effectors in the AKT-mTORC1 pathway: 4EBP1 and 70S6K. However, rapamycin blocked only 70S6K phosphorylation in these cells (Figure 4E), suggesting that phosphorylation and subsequent dissociation of 4EBP1 from the cap-binding translation initiation factor eIF4E might play an important role in regulating HK2 expression. To this end, we introduced tetracycline-inducible non-phosphorylatable 4EBP1 expression system (designed as dominant-negative mutant 4EBP1^M) (Hsieh et al., 2010) into PC3 cells to enhance binding capacity with eIF4E to inhibit cap-dependent translation and observed that induction of 4EBP1^M expression significantly reduced HK2 protein expression (Figure 4F) without affecting HK2 mRNA (Figure S6F). Collectively, our genetic and pharmacological studies support that *Pten* deficiency leads to AKT-mTORC1-mediated phosphorylation of 4EBP1, which then dissociates from eIF4E to activate cap-dependent translation of HK2 mRNA (Figure 4G). In addition, the inability of rapamycin to suppress 4EBP1-HK2 signaling might explain its lack of therapeutic benefits for prostate cancer in experimental and clinical studies.

Loss of p53 Enhances HK2 mRNA through Inhibition of miR143 Biogenesis

In contrast to an early study that wild-type p53 increased HK2 mRNA at the transcription level through p53-responsive elements (Mathupala et al., 1997), we found that loss of p53 significantly upregulated HK2 mRNA in MEFs (Figure 3A) and in prostate epithelial cells (Figure 3C). Conversely, transient exogenous expression of wild-type p53 in PC3 cells significantly reduced HK2 protein expression (Figure 5A) and HK2 mRNA expression (Figure 5B). Induced expression of endogenous p53 in LNCaP cells with genotoxic drug adriamycin (Figure 5D, lane 2 vs. 1), but not in the LNCaP cells in which p53 was silenced by shRNAs (Figure 5D, lane 4 vs. 3; 6 vs. 5), decreased HK2 protein expression (Figure 5D) and HK2 mRNA expression (Figure 5E). Interestingly, no significant induction of HK2 was observed in LNCaP cells with shRNAs to deplete endogenous p53 (Figure 5D, lanes 3 and 5 vs. 1), possibly due to “undetectable” endogenous p53 expression in LNCaP cells and/or other unidentified genetic changes that might contribute to HK2 mRNA regulation. However, these results support that stress-induced wild-type p53 primarily suppresses HK2 mRNA. To support the possibility that the inhibition of HK2 mRNA depended on endogenous p53, we compared p53 wild-type HCT116 and isogenic p53 knockout HCT116 human colon cancer cell lines upon adriamycin challenge and found that reduction of HK2 at mRNA level was only observed in p53 wild-type cells but not in p53 knockout cells (Figures 5G and 5H).

Given that wild-type p53 facilitates the processing of miR143 (Suzuki et al., 2009) and that miR143 destabilizes HK2 mRNA stability in several types of cancer cells (Fang et al., 2012; Gregersen et al., 2012; Jiang et al., 2012; Peschiaroli et al., 2012), we hypothesized that p53 might attenuate HK2 mRNA expression through upregulation of miR-143. Indeed, overexpression of p53 in PC3 cells or induction of endogenous p53 in LNCaP and HCT116

cells dramatically increased miR143 (Figures 5C, 5F, and 5I), correlating with a significant reduction of HK2 mRNA (Figures 5B, 5E, and 5H). To determine causality of suppression of HK2 mRNA through miR143 in prostate cancer cells, we over-expressed miR143 (Figure 5J, lane 2 vs. 1) or administrated miR143 mimic in PC3 cells (Figure 5J, lane 3 vs. 1) and observed much reduced HK2 protein expression (Figure 5J) and concomitant reduction of HK2 mRNA (Figure 5K). These results together suggest that loss of p53 inhibits miR143 biogenesis and relieves miR143-mediated suppression of HK2 mRNA stability, thereby increasing HK2 mRNA (Figure 5L).

HK2 Is Required for *Pten/p53* Deficiency-Driven Prostate Tumor Growth in Xenograft Models

To investigate whether the upregulated HK2 expression in *Pten/p53*-deficient prostate cancer cells is required for the Warburg effect and tumor growth, we knocked down HK2 through stably expressing lentivirus-mediated shRNA in the established mouse *Pten/p53*-deficient prostate cancer cell line (UMN-4240P) (Figure 6A). Efficient knockdown of HK2 in cancer cells led to significant reduction of glucose consumption and lactate production (Figures 6B and 6C), and markedly reduced cell proliferation (Figure 6D). More importantly, depletion of HK2 inhibited anchorage-independent cancer cell growth (Figure 6E) and dramatically attenuated the *in vivo* growth of these xenografted prostate cancer cells in NSG mice (Figure 6F).

To study the essential role of elevated HK2 in human *Pten/p53*-deficient prostate cancer cells, we generated two stable cell lines in PC3 cells with varying degrees of reduction of HK2 expression: shHK202, which robustly decreased total HK2 protein, and shHK201, which reduced HK2 by a lesser degree (Figure 6I). Depletion of HK2 in these two PC3 cell lines resulted in significantly reduced glucose consumption and lactate production (Figures 6J and 6K), attenuated their colony growth (Figure 6L), and inhibited anchorage-independent cell growth examined by soft-agar assay (Figures 6M and 6N). Furthermore, the growth of xenografted PC3 cells stably expressing shHK2-01 or shHK2-02 in NSG mice was significantly suppressed compared to PC3 cells with a scramble shRNA (Figure 6O). When necropsied at 4 weeks after subcutaneous inoculation, tumors that derived from scrambled shRNA-expressing cells grew to an average weight of 155mg, whereas tumors that derived from shHK2-01- and shHK2-02-expressing cells grew to an average weight of 55mg and 20mg, respectively (Figure 6O). Importantly, the magnitude of reduction in tumor weight as well as in *in vitro* growth indices reflected the efficiency of the HK2 knockdown in PC3 cells.

We then examined the cellular processes underlying the suppression of tumor growth in xenograft mouse models carrying HK2-depleted prostate cancer cells. Knockdown of HK2 in UMN-4240P mouse *Pten/p53*-deficient prostate cancer cells decreased cell proliferation as indicated by the significant reduction of positive staining of cellular proliferation marker Ki67 (Figures 6G and 6H). Identical results were observed in xenograft harboring human *Pten/p53*-deficient prostate cancer PC3 cells (Figures 6P and 6Q). However, HK2 depletion did not induce significant apoptosis since we found minimal changes in the proportion of cells with cleaved caspase 3 (Data not shown). These data suggest that the impaired ability

of HK2-depleted cells to develop into tumors is primarily due to inhibition of cancer cell proliferation. Taken together, the xenograft studies provided genetic evidence that the *Pten/p53*-deficient prostate cancer cells require HK2-mediated glycolysis to fuel tumor growth *in vivo*.

HK2 Is Expressed in Human Prostate Cancer

Previous studies indicated that HK2 expression was observed in several types of human tumor specimens, including glioblastoma multiforme (GBM) (Wolf et al., 2011), lung, and breast cancer samples (Patra et al., 2013). We did immunoblotting to examine HK2 and HK1 expression in normal human prostate tissues and cancer specimens. HK2 was exclusively expressed in prostate cancers, whereas HK1 expression was observed in both normal and cancerous tissues (Figure 7A). We then analyzed tumor tissue microarray (TMA) of human prostate cancer by immunohistochemistry (IHC) and observed that HK2 expression was significantly elevated in prostate tumor samples compared with normal prostate tissue, although the protein expression level of HK2 was highly variable among individual tumors (Figures 7B–7D). Importantly, a significant correlation between HK2 protein expression and Gleason score was detected (Figures 7E and 7F).

To explore whether the extent of HK2-specific alteration in prostate cancer correlates with *Pten* and *p53* loss/mutations, we analyzed TMA for PTEN, p53 and HK2 expressions by IHC (Figure 7G). Since expression of wild-type p53 protein was hardly detectable by IHC, negative staining of p53 could not be distinguished from cancer cells carrying wild-type p53 or p53 deletions. We therefore focused on nuclear protein accumulation of p53, a hallmark of the presence of *p53* missense mutations that contribute to more than 85% of p53 mutations identified in human cancers (Muller and Vousden, 2014). Indeed, a high level of HK2 expression was observed in 8 out of 9 tumor samples with negative staining of PTEN and positive staining of mutant p53 (Figures 7G and S7), suggesting combined deletion/mutation of *Pten* and *p53* contributes to the elevated HK2 expression in human prostate cancer.

Discussion

Recent studies suggest that tumor suppressor gene inactivation alters glucose metabolism to favor the Warburg effect, which in turn plays a causal role in tumorigenesis (Levine and Puzio-Kuter, 2010). In our study, HK2 is almost exclusively expressed in prostate cancer tissue in comparison with normal prostate tissue (Figure 7A) and its protein expression level positively correlates with Gleason score (Figures 7E and 7F). Although limited by 9 informative cases, a high level of HK2 expression has been observed in 8 prostate cancer samples with negative staining of PTEN and positive staining of mutant p53 (Figures 7G and S8). Importantly, genetic studies demonstrate that HK2-mediated Warburg effect is required for the growth of *Pten/p53*-deficient prostate cancer cells *in vitro* and in xenograft models carrying mouse or human *Pten/p53*-deficient prostate cancer cell lines *in vivo* (Figure 6). These results are consistent with a previous study of glioblastoma that showed HK2 depletion by shRNAs inhibits tumor growth in a xenograft model (Wolf et al., 2011). More recently, a study using HK2 conditional knockout mice shows that HK2 is required for

tumor initiation and maintenance in mouse models of *Kras*-driven lung cancer and *ErbB2*-driven breast cancer (Patra et al., 2013). Our study extended the biological significance of HK2 to *Pten/p53*-deficient prostate cancers, which are particularly relevant to the treatment of current incurable metastatic CRPC for which taxane-based chemotherapeutics and/or androgen- and/or androgen receptor-targeted molecular therapies have limited efficacy. These findings therefore provide a novel therapeutic strategy for CRPC by targeting its heightened HK2-mediated glycolysis.

Although increased HK2 expression has been observed in cancer cells and tumor tissues from mouse models or patients (Patra et al., 2013; Wolf et al., 2011), our current study provides significant novel insights into the underlying molecular mechanisms for HK2 overexpression in cancer cells carrying *Pten/p53* aberrations. Upon AKT activation, HK2 protein undergoes mitochondrial translocation (Majewski et al., 2004) through AKT-mediated HK2 phosphorylation (Roberts et al., 2013). At the transcriptional level, activation of the AKT-mTOR pathway upregulates HK2 mRNA expression through induction of and enhancement of hypoxia-inducible factors (HIFs) binding to the HK2 promoter (Mathupala et al., 2001). We here demonstrate that activation of the AKT-mTORC1 signaling due to *Pten* deletion increases HK2 expression primarily at the translational level through phosphorylation of the 4EBP1 signaling. To recap the key data, we have shown that loss of *Pten* in MEFs or in prostate epithelium (Figures 3A and 3C) does not increase HK2 mRNA level, yet enhances HK2 protein level (Figures 2G–2I). *Pten* deletion in p53-deficient cells dramatically increases HK2 protein expression (Figures 1C and 2) without further induction of HK2 mRNA over that induced by p53-deletion alone (Figures 3A and 3C), but instead with a significant enhancement of polysome-associated HK2 mRNA (Figure 4B). Conversely, shRNA-mediated inhibition of the AKT-mTORC1 signaling by depletion of AKT or Raptor decreases HK2 protein expression without reduction of HK2 mRNA level (Figure 3), but rather through a significant reduction of polysome-associated HK2 mRNA (Figures 4C and 4D). Active mTORC1 complex phosphorylates 4E-BP1, which is therefore unable to bind to eIF4E. Thus, eIF4E is free to bind to eIF4G, which forms the eIF4F complex on the 5' cap of mRNA and initiates translation (Laplanche and Sabatini, 2012). In support of the critical role of phosphorylated 4EBP1 in regulation of HK2 mRNA translation, we showed that the PI3K-mTOR dual inhibitor NVP-BEZ235, but not the allosteric mTORC1 inhibitor rapamycin, significantly reduces HK2 protein expression complying with a marked inhibition of 4EBP1 phosphorylation (Figure 4E). More importantly, doxycycline-induced expression of dominant-negative mutant of 4EBP1 (4EBP1^M) (Hsieh et al., 2010), which tightly binds to eIF4E due to reduction of phosphorylation, significantly suppresses HK2 protein but not HK2 mRNA (Figures 4F and S6F). These findings support that phosphorylated 4EBP1-mediated cap-dependent translation is essential for the induction of HK2 protein in prostate cancer cells harboring *Pten* deletion.

In reference to p53, an early study suggested that p53 increases HK2 mRNA transcription through p53-responsive elements (Mathupala et al., 1997). In contrast, we observed that loss of p53 enhances HK2 mRNA expression in our experimental settings (Figure 3). We have shown that exogenous expression of wild type p53 in p53-null prostate cancer cells reduces

HK2 mRNA expression (Figure 5) and that genotoxic drug adriamycin-induced endogenous p53 expression in p53-wild type cancer cells, but not in p53-deficient cancer cells, suppresses HK2 mRNA, supporting p53 induction is required for the reduction of HK2 mRNA (Figure 5). Mechanistically, we demonstrated that loss of p53 decreases the biogenesis of miR143, which in turn leads to degradation of HK2 mRNA through binding the 3'UTR. By over-expression of miR143 or administration of miR143 mimics in p53-deficient prostate cancer cells, we observed significant reduction of HK2 mRNA (Figure 5K), in support of miR143's role as a direct effector to target HK2. These results collectively indicate that the loss of p53 in prostate cancer cells enhances HK2 protein expression by removal of miR143-mediated degradation of HK2 mRNA.

In summary, our findings support that HK2 is co-regulated by the p53-miR143 axis at the mRNA/posttranscriptional level and by the PTEN-AKT-mTOR-4EBP1 signaling at the protein/translational level. As a result, the combined deficiency of *Pten* and *p53* in prostate cancer cells synergistically leads to robustly elevated HK2 expression to fuel the aggressive prostate cancer growth *in vivo*.

Experimental Procedures

Pten and/or *p53* Mutant Mice

The conditional *Pten*^{flox/flox} mouse was generated as previously described (Zheng et al., 2008). The conditional *p53*^{flox/flox} mouse was generously provided by Dr. A Berns (Jonkers et al., 2001). *PB-Cre4* transgenic mice were obtained from the NCI Mouse Repository. Female mice carrying *Pten*^{flox/+}*p53*^{flox/+} were crossed with male mice harboring *PB-Cre4*⁺*Pten*^{flox/+}*p53*^{flox/+} to generate mutant mice with prostate epithelium-specific deletion of *Pten* and/or *p53*. Tail DNA was used for PCR-based genotyping. All animal protocols were reviewed and approved by the University of Minnesota Institutional Animal Care and Use Committee.

Generation of MEFs with Conditional Deletion of *Pten* and/or *p53*

MEFs were generated from 13.5-day embryos of a *Pten*^{Flox/+}, *p53*^{Flox/+} and *Pten*^{Flox/+}, *p53*^{Flox/+} mating. To delete *Pten* and/or *p53*, primary MEFs with floxed *Pten* alleles and/or floxed *p53* alleles were transduced with a lentiviral vector carrying Cre. Deletion of *Pten* and/or *p53* was confirmed by both PCR and Western blot.

Generation of Prostate Cancer Cell lines

The prostate tumors derived from mice carrying *PB-Cre4*⁺*Pten*^{flox/flox}*p53*^{flox/flox} were surgically removed and digested with collagenase solution (Stemcell Technologies) at 37°C. Digested tumors were washed 3 times with PBS to remove collagenase. The cell pellets were then suspended in DMEM containing 10% FBS, and cells were grown at standard tissue culture condition. Stable polyclonal tumor cell lines (UMN-4240P) were expanded for one to two generations and frozen down for future experiments. Deletion of *Pten* and *p53* in prostate cancer cell line was verified by both PCR and Western blot.

Statistical Analyses

Statistical comparisons were analyzed by ANOVA (greater than 2 groups) or Student's *t* test (2 groups only) with Graphad Prism (v.5). Mann-Whitney *U* test was used to assess differences of HK2 expression in human prostate cancers. Spearman's ρ was used to assess correlation. Statistical significances were accepted at $p < 0.05$.

Supplementary Material

Refer to Web version on PubMed Central for supplementary material.

Acknowledgments

This work is supported, in part, by grants from the US National Cancer Institute (K01 CA124461, Y.D.; R01 CA160333, Y.D.; R21 CA155522, Y.D. and J.L.; R01 CA172169, J.L. and Y.D.; R01 CA130908, H.H.; R01 CA164346, M.J.Y.), The University of Minnesota Grant-in Aid (Y.D.) and start-up funds from The Hormel Foundation (Y.D.).

References

- Barbieri CE, Baca SC, Lawrence MS, Demichelis F, Blattner M, Theurillat JP, White TA, Stojanov P, Van Allen E, Stransky N, et al. Exome sequencing identifies recurrent SPOP, FOXA1 and MED12 mutations in prostate cancer. *Nat Genet.* 2012; 44:685–689. [PubMed: 22610119]
- Bensaad K, Tsuruta A, Selak MA, Vidal MN, Nakano K, Bartrons R, Gottlieb E, Vousden KH. TIGAR, a p53-inducible regulator of glycolysis and apoptosis. *Cell.* 2006; 126:107–120. [PubMed: 16839880]
- Cairns P, Okami K, Halachmi S, Halachmi N, Esteller M, Herman JG, Jen J, Isaacs WB, Bova GS, Sidransky D. Frequent inactivation of PTEN/MMAC1 in primary prostate cancer. *Cancer Res.* 1997; 57:4997–5000. [PubMed: 9371490]
- Chen ML, Xu PZ, Peng XD, Chen WS, Guzman G, Yang X, Di Cristofano A, Pandolfi PP, Hay N. The deficiency of Akt1 is sufficient to suppress tumor development in Pten^{+/-} mice. *Genes Dev.* 2006; 20:1569–1574. [PubMed: 16778075]
- Chen Z, Trotman LC, Shaffer D, Lin HK, Dotan ZA, Niki M, Koutcher JA, Scher HI, Ludwig T, Gerald W, et al. Crucial role of p53-dependent cellular senescence in suppression of Pten-deficient tumorigenesis. *Nature.* 2005; 436:725–730. [PubMed: 16079851]
- DeMarzo AM, Nelson WG, Isaacs WB, Epstein JI. Pathological and molecular aspects of prostate cancer. *Lancet.* 2003; 361:955–964. [PubMed: 12648986]
- Fang M, Shen Z, Huang S, Zhao L, Chen S, Mak TW, Wang X. The ER UDPase ENTPD5 promotes protein N-glycosylation, the Warburg effect, and proliferation in the PTEN pathway. *Cell.* 2010; 143:711–724. [PubMed: 21074248]
- Fang R, Xiao T, Fang Z, Sun Y, Li F, Gao Y, Feng Y, Li L, Wang Y, Liu X, et al. MicroRNA-143 (miR-143) regulates cancer glycolysis via targeting hexokinase 2 gene. *The Journal of biological chemistry.* 2012; 287:23227–23235. [PubMed: 22593586]
- Grasso CS, Wu YM, Robinson DR, Cao X, Dhanasekaran SM, Khan AP, Quist MJ, Jing X, Lonigro RJ, Brenner JC, et al. The mutational landscape of lethal castration-resistant prostate cancer. *Nature.* 2012; 487:239–243. [PubMed: 22722839]
- Gray IC, Phillips SM, Lee SJ, Neoptolemos JP, Weissenbach J, Spurr NK. Loss of the chromosomal region 10q23-25 in prostate cancer. *Cancer Res.* 1995; 55:4800–4803. [PubMed: 7585509]
- Gregersen LH, Jacobsen A, Frankel LB, Wen J, Krogh A, Lund AH. MicroRNA-143 down-regulates Hexokinase 2 in colon cancer cells. *BMC cancer.* 2012; 12:232. [PubMed: 22691140]
- Guertin DA, Sabatini DM. Defining the role of mTOR in cancer. *Cancer Cell.* 2007; 12:9–22. [PubMed: 17613433]

- Haffner MC, Mosbrugger T, Esopi DM, Fedor H, Heaphy CM, Walker DA, Adejola N, Gurel M, Hicks J, Meeker AK, et al. Tracking the clonal origin of lethal prostate cancer. *J Clin Invest*. 2013; 123:4918–4922. [PubMed: 24135135]
- Hsieh AC, Costa M, Zollo O, Davis C, Feldman ME, Testa JR, Meyuhos O, Shokat KM, Ruggero D. Genetic dissection of the oncogenic mTOR pathway reveals druggable addiction to translational control via 4EBP-eIF4E. *Cancer Cell*. 2010; 17:249–261. [PubMed: 20227039]
- Hu W, Zhang C, Wu R, Sun Y, Levine A, Feng Z. Glutaminase 2, a novel p53 target gene regulating energy metabolism and antioxidant function. *Proc Natl Acad Sci U S A*. 2010; 107:7455–7460. [PubMed: 20378837]
- Jacinto E, Facchinetti V, Liu D, Soto N, Wei S, Jung SY, Huang Q, Qin J, Su B. SIN1/MIP1 maintains rictor-mTOR complex integrity and regulates Akt phosphorylation and substrate specificity. *Cell*. 2006; 127:125–137. [PubMed: 16962653]
- Jiang P, Du W, Wang X, Mancuso A, Gao X, Wu M, Yang X. p53 regulates biosynthesis through direct inactivation of glucose-6-phosphate dehydrogenase. *Nat Cell Biol*. 2011; 13:310–316. [PubMed: 21336310]
- Jiang S, Zhang LF, Zhang HW, Hu S, Lu MH, Liang S, Li B, Li Y, Li D, Wang ED, Liu MF. A novel miR-155/miR-143 cascade controls glycolysis by regulating hexokinase 2 in breast cancer cells. *The EMBO journal*. 2012; 31:1985–1998. [PubMed: 22354042]
- Jonkers J, Meuwissen R, van der Gulden H, Peterse H, van der Valk M, Berns A. Synergistic tumor suppressor activity of BRCA2 and p53 in a conditional mouse model for breast cancer. *Nat Genet*. 2001; 29:418–425. [PubMed: 11694875]
- Kondoh H, Leonart ME, Gil J, Wang J, Degan P, Peters G, Martinez D, Carnero A, Beach D. Glycolytic enzymes can modulate cellular life span. *Cancer Res*. 2005; 65:177–185. [PubMed: 15665293]
- Levine AJ, Puzio-Kuter AM. The control of the metabolic switch in cancers by oncogenes and tumor suppressor genes. *Science*. 2010; 330:1340–1344. [PubMed: 21127244]
- Lunardi A, Ala U, Epping MT, Salmena L, Clohessy JG, Webster KA, Wang G, Mazzucchelli R, Bianconi M, Stack EC, et al. A co-clinical approach identifies mechanisms and potential therapies for androgen deprivation resistance in prostate cancer. *Nat Genet*. 2013; 45:747–755. [PubMed: 23727860]
- Majewski N, Nogueira V, Bhaskar P, Coy PE, Skeen JE, Gottlob K, Chandel NS, Thompson CB, Robey RB, Hay N. Hexokinase-mitochondria interaction mediated by Akt is required to inhibit apoptosis in the presence or absence of Bax and Bak. *Molecular cell*. 2004; 16:819–830. [PubMed: 15574336]
- Markert EK, Mizuno H, Vazquez A, Levine AJ. Molecular classification of prostate cancer using curated expression signatures. *Proc Natl Acad Sci U S A*. 2011; 108:21276–21281. [PubMed: 22123976]
- Mathupala SP, Heese C, Pedersen PL. Glucose catabolism in cancer cells. The type II hexokinase promoter contains functionally active response elements for the tumor suppressor p53. *The Journal of biological chemistry*. 1997; 272:22776–22780. [PubMed: 9278438]
- Mathupala SP, Rempel A, Pedersen PL. Glucose catabolism in cancer cells: identification and characterization of a marked activation response of the type II hexokinase gene to hypoxic conditions. *The Journal of biological chemistry*. 2001; 276:43407–43412. [PubMed: 11557773]
- Matoba S, Kang JG, Patino WD, Wragg A, Boehm M, Gavrilova O, Hurley PJ, Bunz F, Hwang PM. p53 regulates mitochondrial respiration. *Science*. 2006; 312:1650–1653. [PubMed: 16728594]
- Muller PA, Vousden KH. Mutant p53 in Cancer: New Functions and Therapeutic Opportunities. *Cancer Cell*. 2014; 25:304–317. [PubMed: 24651012]
- Navone NM, Labate ME, Troncoso P, Pisters LL, Conti CJ, von Eschenbach AC, Logothetis CJ. p53 mutations in prostate cancer bone metastases suggest that selected p53 mutants in the primary site define foci with metastatic potential. *J Urol*. 1999; 161:304–308. [PubMed: 10037428]
- Patra KC, Wang Q, Bhaskar PT, Miller L, Wang Z, Wheaton W, Chandel N, Laakso M, Muller WJ, Allen EL, et al. Hexokinase 2 Is Required for Tumor Initiation and Maintenance and Its Systemic Deletion Is Therapeutic in Mouse Models of Cancer. *Cancer Cell*. 2013; 24:213–228. [PubMed: 23911236]

- Peschiaroli A, Giacobbe A, Formosa A, Markert EK, Bongiorno-Borbone L, Levine AJ, Candi E, D'Alessandro A, Zolla L, Finazzi Agro A, Melino G. miR-143 regulates hexokinase 2 expression in cancer cells. *Oncogene*. 2012; 32:797–802. [PubMed: 22469988]
- Roberts DJ, Tan-Sah VP, Smith JM, Miyamoto S. Akt phosphorylates HK-II at Thr-473 and increases mitochondrial HK-II association to protect cardiomyocytes. *The Journal of biological chemistry*. 2013; 288:23798–23806. [PubMed: 23836898]
- Sarbassov DD, Guertin DA, Ali SM, Sabatini DM. Phosphorylation and regulation of Akt/PKB by the rictor-mTOR complex. *Science*. 2005; 307:1098–1101. [PubMed: 15718470]
- Shen MM, Abate-Shen C. Molecular genetics of prostate cancer: new prospects for old challenges. *Genes Dev*. 2010; 24:1967–2000. [PubMed: 20844012]
- Song MS, Salmena L, Pandolfi PP. The functions and regulation of the PTEN tumour suppressor. *Nat Rev Mol Cell Biol*. 2012; 13:283–296. [PubMed: 22473468]
- Sun Q, Chen X, Ma J, Peng H, Wang F, Zha X, Wang Y, Jing Y, Yang H, Chen R, et al. Mammalian target of rapamycin up-regulation of pyruvate kinase isoenzyme type M2 is critical for aerobic glycolysis and tumor growth. *Proc Natl Acad Sci U S A*. 2011; 108:4129–4134. [PubMed: 21325052]
- Suzuki H, Freije D, Nusskern DR, Okami K, Cairns P, Sidransky D, Isaacs WB, Bova GS. Interfocal heterogeneity of PTEN/MMAC1 gene alterations in multiple metastatic prostate cancer tissues. *Cancer Res*. 1998; 58:204–209. [PubMed: 9443392]
- Suzuki HI, Yamagata K, Sugimoto K, Iwamoto T, Kato S, Miyazono K. Modulation of microRNA processing by p53. *Nature*. 2009; 460:529–533. [PubMed: 19626115]
- Suzuki S, Tanaka T, Poyurovsky MV, Nagano H, Mayama T, Ohkubo S, Lokshin M, Hosokawa H, Nakayama T, Suzuki Y, et al. Phosphate-activated glutaminase (GLS2), a p53-inducible regulator of glutamine metabolism and reactive oxygen species. *Proc Natl Acad Sci U S A*. 2010; 107:7461–7466. [PubMed: 20351271]
- Whang YE, Wu X, Suzuki H, Reiter RE, Tran C, Vessella RL, Said JW, Isaacs WB, Sawyers CL. Inactivation of the tumor suppressor PTEN/MMAC1 in advanced human prostate cancer through loss of expression. *Proc Natl Acad Sci U S A*. 1998; 95:5246–5250. [PubMed: 9560261]
- Wilson JE. Isozymes of mammalian hexokinase: structure, subcellular localization and metabolic function. *The Journal of experimental biology*. 2003; 206:2049–2057. [PubMed: 12756287]
- Wolf A, Agnihotri S, Micallef J, Mukherjee J, Sabha N, Cairns R, Hawkins C, Guha A. Hexokinase 2 is a key mediator of aerobic glycolysis and promotes tumor growth in human glioblastoma multiforme. *The Journal of experimental medicine*. 2011; 208:313–326. [PubMed: 21242296]
- Wu X, Wu J, Huang J, Powell WC, Zhang J, Matusik RJ, Sangiorgi FO, Maxson RE, Sucov HM, Roy-Burman P. Generation of a prostate epithelial cell-specific Cre transgenic mouse model for tissue-specific gene ablation. *Mech Dev*. 2001; 101:61–69. [PubMed: 11231059]
- Zhang C, Lin M, Wu R, Wang X, Yang B, Levine AJ, Hu W, Feng Z. Parkin, a p53 target gene, mediates the role of p53 in glucose metabolism and the Warburg effect. *Proc Natl Acad Sci U S A*. 2011; 108:16259–16264. [PubMed: 21930938]
- Zheng H, Ying H, Yan H, Kimmelman AC, Hiller DJ, Chen AJ, Perry SR, Tonon G, Chu GC, Ding Z, et al. p53 and Pten control neural and glioma stem/progenitor cell renewal and differentiation. *Nature*. 2008; 455:1129–1133. [PubMed: 18948956]

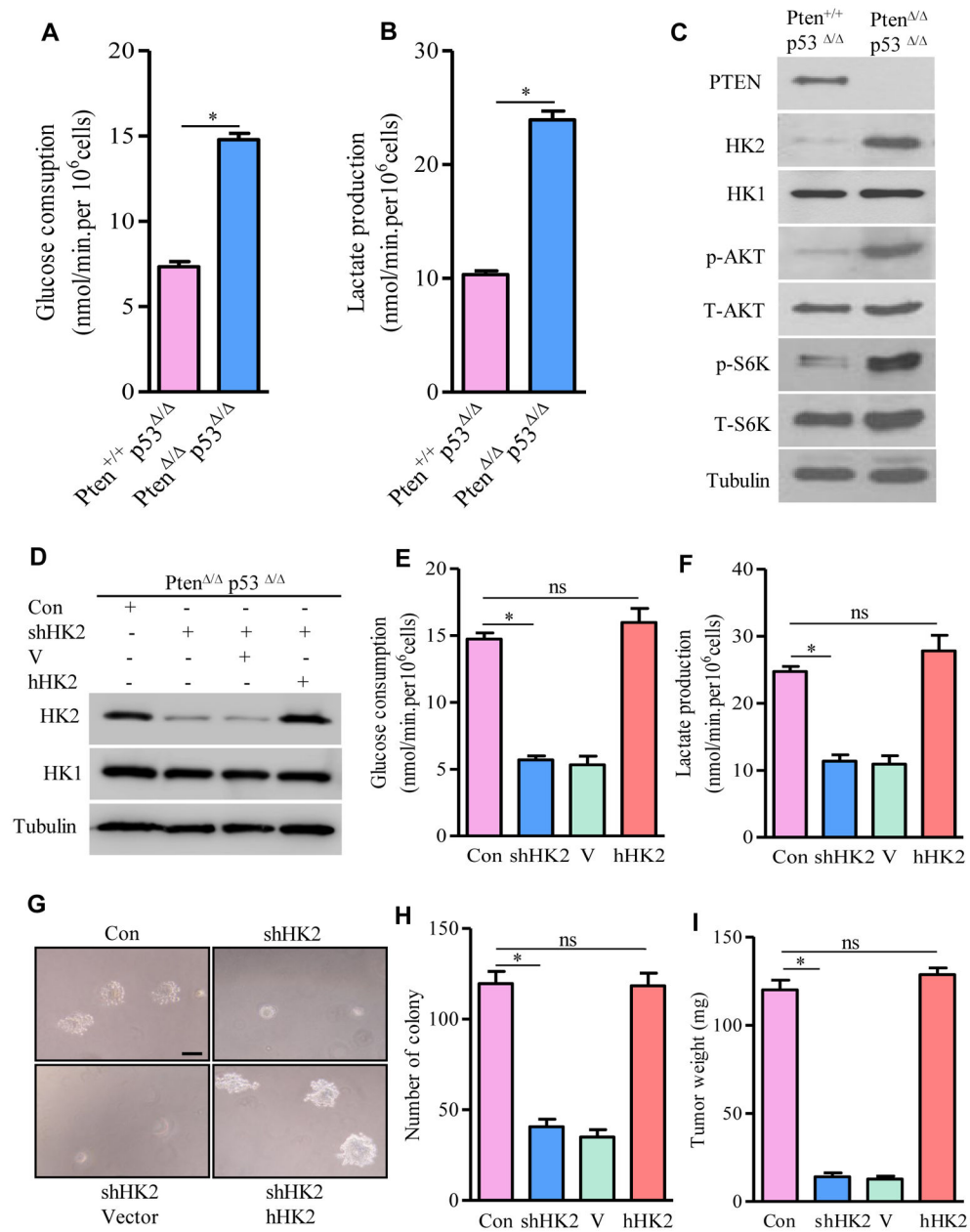


Figure 1. HK2-Mediated Warburg Effect Is Required for Tumorigenesis in *Pten/p53*-Deficient MEFs

(A and B) Glucose consumption (A) and lactate production (B) in *Pten*^{+/+}*p53*^{Δ/Δ} and *Pten*^{Δ/Δ}*p53*^{Δ/Δ} MEFs. (C) Lysates from *Pten*^{+/+}*p53*^{Δ/Δ} and *Pten*^{Δ/Δ}*p53*^{Δ/Δ} MEFs were immunoblotted by the indicated antibodies. (D) Lysates from *Pten*^{Δ/Δ}*p53*^{Δ/Δ} MEFs carrying shRNA for mouse HK2 or expressing human HK2 were determined by Western blotting. (E and F) Glucose consumption (E) and lactate production (F) in HK2-depleted or human HK2 rescued *Pten*^{Δ/Δ}*p53*^{Δ/Δ} MEFs. (G) Representative images of HK2-deficient or human HK2-rescued MEFs growing in soft-agar. (H) Quantification of macroscopic colonies in G from three independent experiments. (I) Weight of tumors developed from NOD/SCID IL2RG mice carrying HK2-deficient or human HK2-rescued *Pten*^{Δ/Δ}*p53*^{Δ/Δ} MEFs. For Western

blots, tubulin was used as a loading control. All data in the graph bars are means \pm SEM. * P < 0.001. ns: not statistically significant. Scale bar: 100um. See also Figures S1 and S2.

Author Manuscript

Author Manuscript

Author Manuscript

Author Manuscript

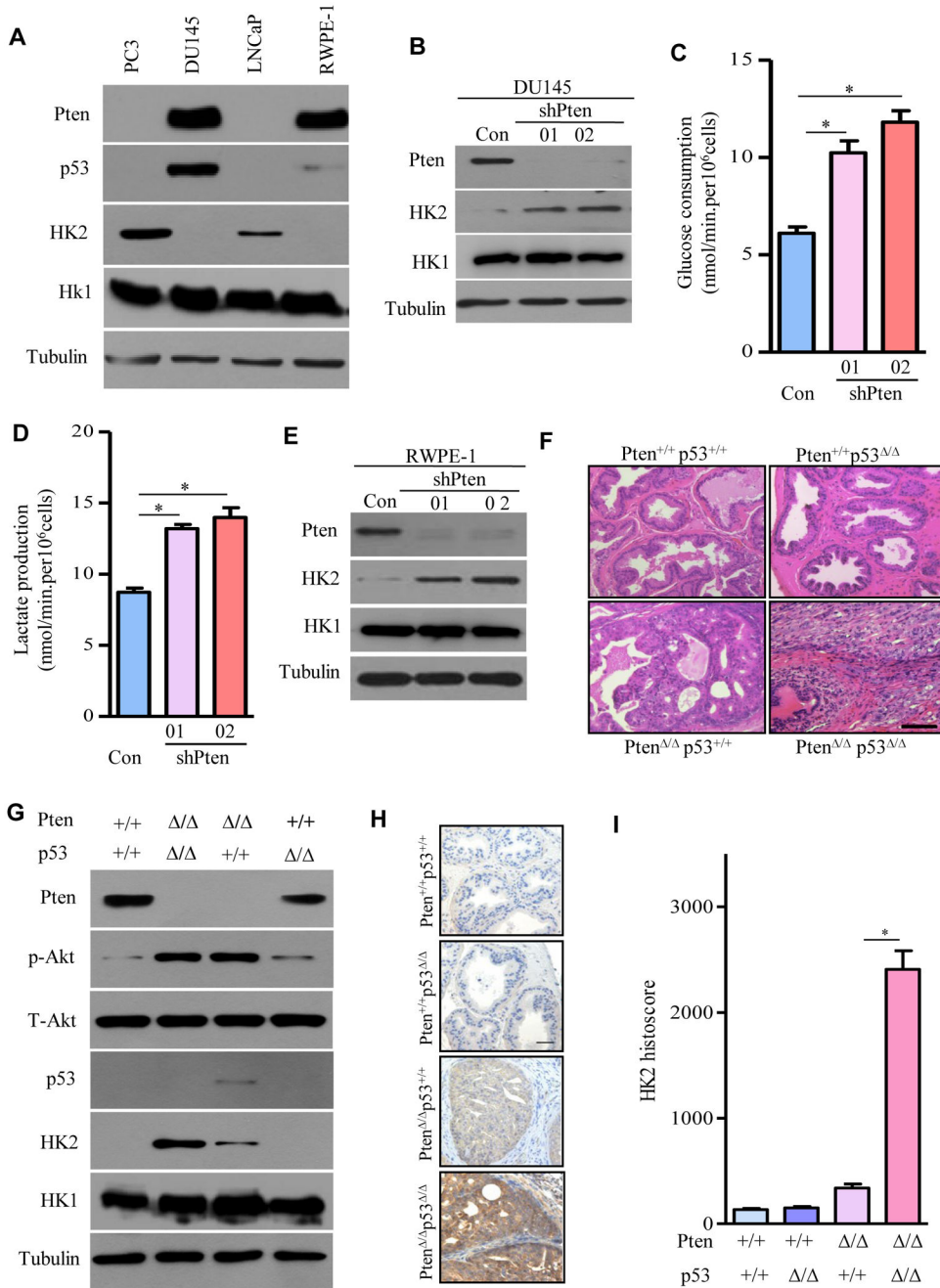


Figure 2. HK2 Protein Expression Is Elevated in *Pten/p53*-Deficient Prostate Cancer Cells
 (A) Lysates from human prostate cancer cell lines and untransformed human prostate epithelial cells were immunoblotted by the indicated antibodies. (B) Protein levels of Pten, HK2, and HK1 were detected by Western blotting in DU145 cells expressing shRNAs for Pten. (C and D) Glucose consumption (C) and lactate production (D) in Pten-depleted DU145 cells. (E) Protein levels of Pten, HK2, and HK1 were determined by Western in RWPE-1 cells expressing shRNAs for Pten. (F) Representative images of Haematoxylin/Eosin staining of prostate from the indicated genotypes. (G) Extracts from prostate of 20-week-old mice of the identified genotypes were immunoblotted by the indicated antibodies. (H) IHC images of HK2 in the indicated genotypes. (I) HK2 histoscore in the indicated genotypes.

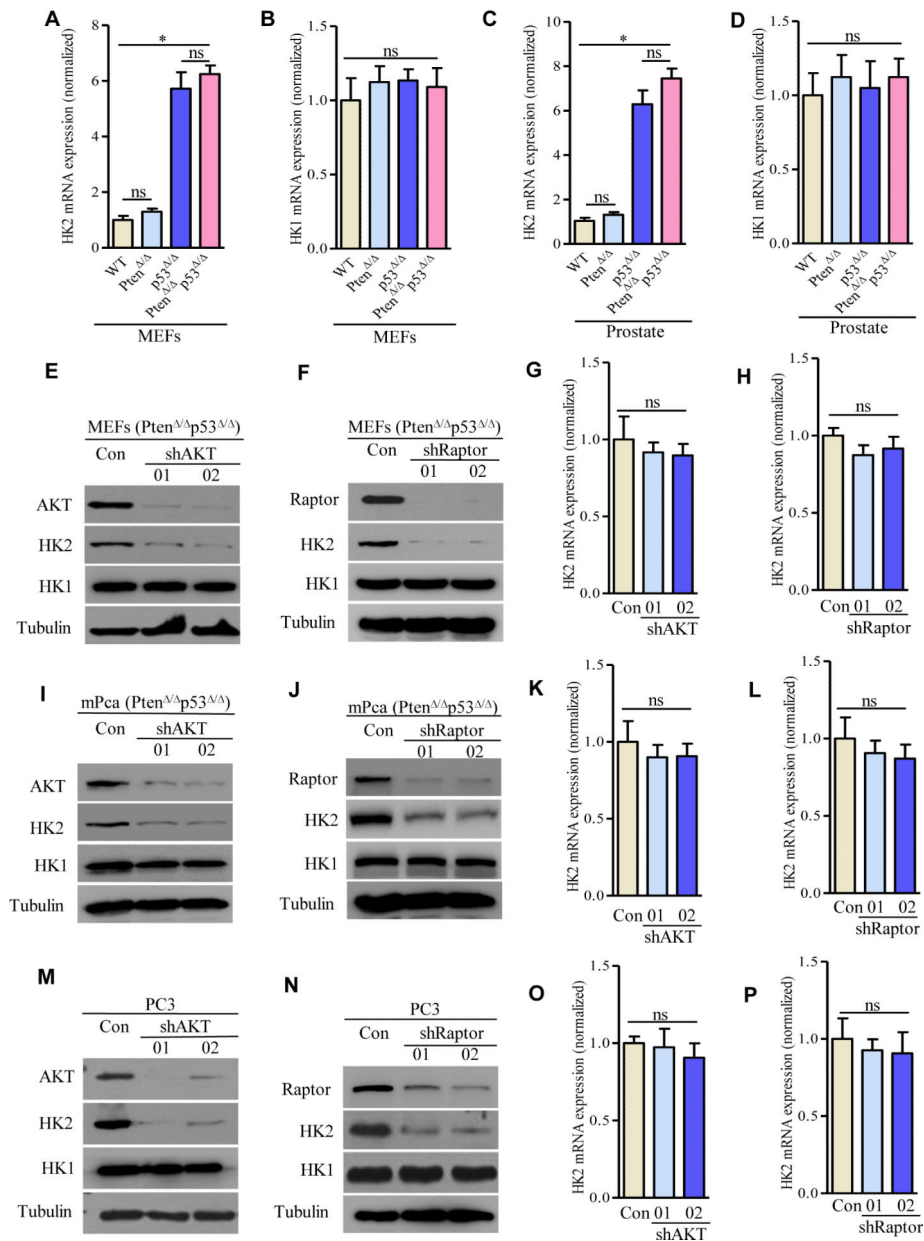
(H) Representative IHC images of HK2-stained prostate epithelium with the indicated genotype were shown. (I) Quantification of HK2 IHC staining was performed with Image-Pro plus (v 6.3) and shown in bar graphs. For Western blots, tubulin was used as a loading control. All data in the graph bars represent means \pm SEM. *P \leq 0.01. Scale bar: 100um. See also Figures S3–S5.

Author Manuscript

Author Manuscript

Author Manuscript

Author Manuscript



loading control. All data are means \pm SEM. *P < 0.01. ns: not statistically significant. See also Figure S6.

Author Manuscript

Author Manuscript

Author Manuscript

Author Manuscript

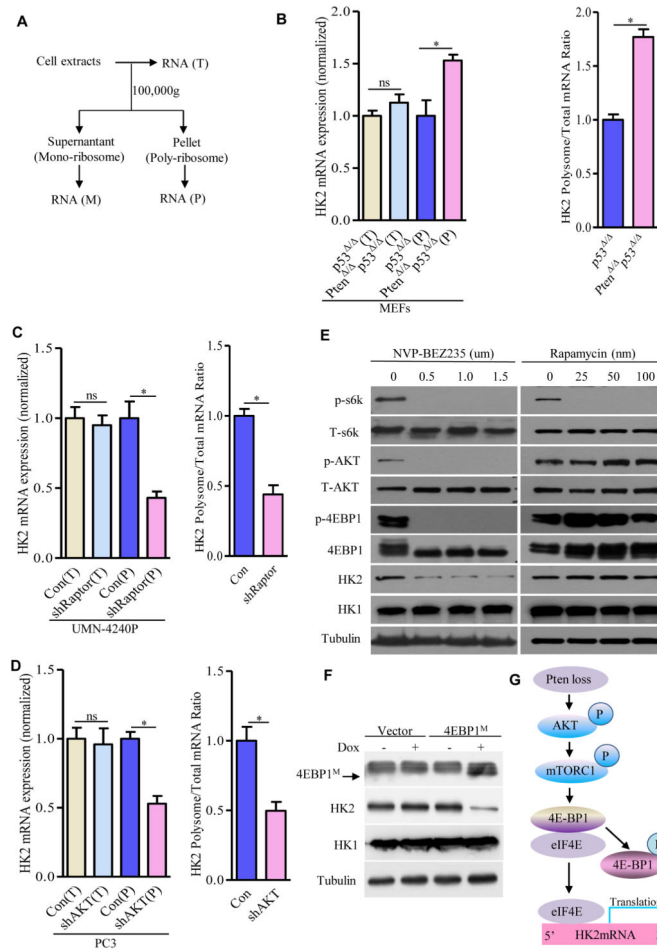


Figure 4. Pten Deficiency Translationally Upregulates HK2 through Phosphorylation of 4E-BP1 (A) Schematic presentation of total, monoriobosomal, and polysomal mRNA distribution after different centrifugation. (B–D) Real time RT-PCR analysis of total HK2 mRNA levels and the HK2 mRNA loaded on polysomes (left panel) in MEFs carrying *p53*^{+/+} or *Pten*^{+/+}*p53*^{+/+} (B), in *Pten/p53*-deficient mouse prostate cancer UMN-4240P cells expressing shRNA for Raptor (C), or in *Pten/p53*-deficient human prostate cancer PC3 cells expressing shRNA for AKT (D). The respective right panel shows the ratio between the level of HK2 mRNA loaded on the polysome and the total HK2 mRNA. Note that each value was normalized to total β-actin expression and β-actin loaded on the polysome. (E and F) Phosphorylation of 4EBP1 regulates HK2 expression. Immunoblots of lysates from PC3 cells were treated with NVP-BEZ235 or rapamycin at the indicated doses for 36 hr (E), and HK2 expression was determined by Western blotting from PC3 cells expressing tetracycline-inducible dominant-negative mutant 4EBP1M after 48 hr doxycycline (1ug/ml) treatment (F). (G) Schematic model addressing HK2 upregulation upon *Pten* deletion. For Western blots, tubulin was used as a loading control. All data are means ± SEM. *P < 0.01. ns: not statistically significant. See also Figure S6.

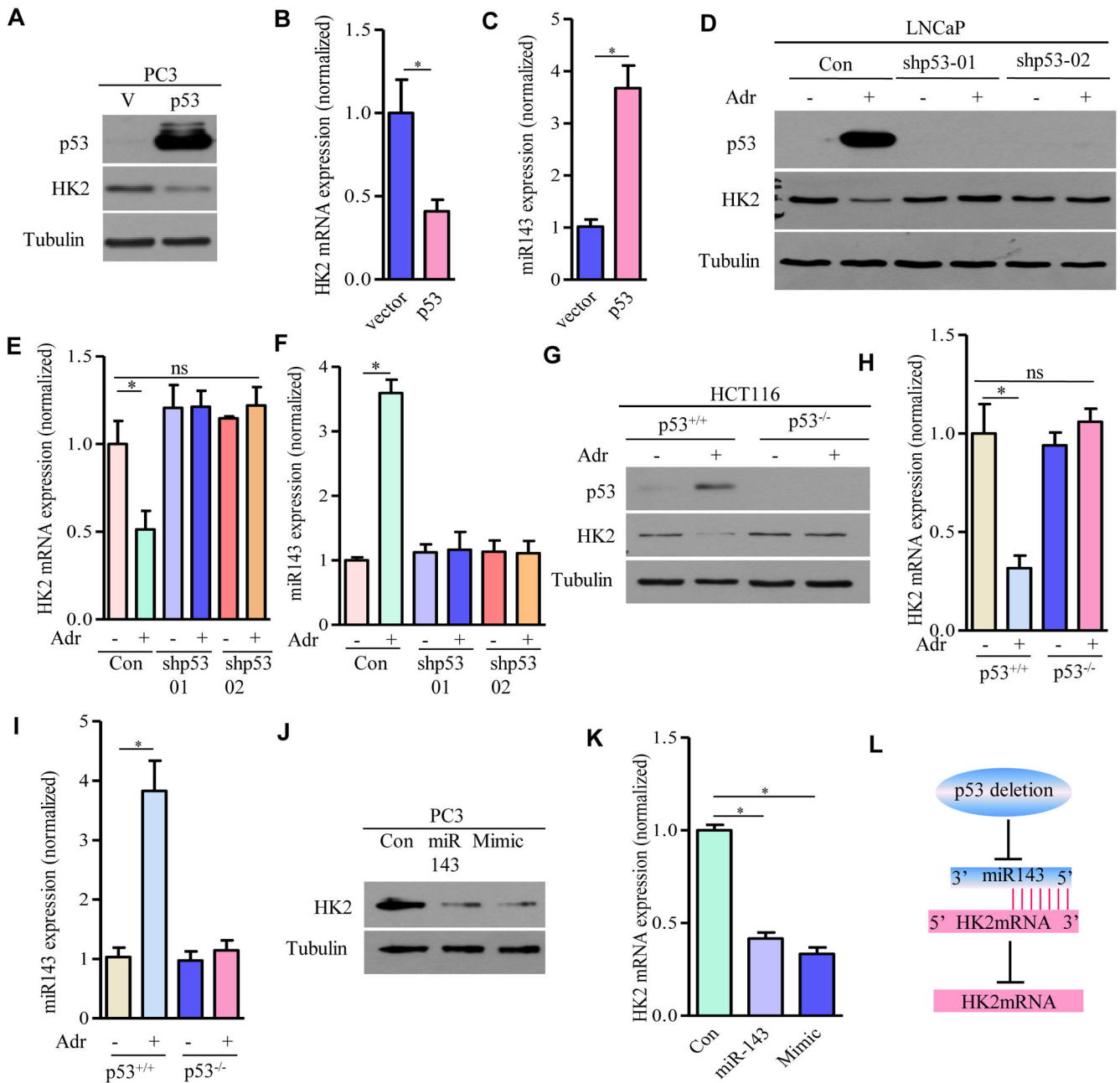


Figure 5. p53 Deletion Upregulates HK2 mRNA through Inhibition of miR143 Biogenesis
 (A–C) p53 regulates miR-143 and HK2 in PC3 cells. HK2 protein (A), HK2 mRNA levels (B) and miR-143 (C) were examined by Western blotting or real-time RT-PCR in PC3 cells expressing wild type p53. (D–F) Effects of shRNA knockdown of p53 on HK2 and miR143 expression in adriamycin-treated LNCaP cells: HK2 protein levels (D) were detected by Western blot, HK2 mRNA (E) and miR-143 (F) were measured by real time RT-PCR and shown as means \pm SEM (n = 3). (G–I) Effects of p53 knockout on HK2 and miR143 expression in adriamycin-treated HCT116 cells: HK2 protein levels were examined by Western blot (G), HK2 mRNA (H) and miR143 (I) were examined by real RT-PCR and

shown as means \pm SEM (n = 3). (J and K) Effects of miR-143 on HK2 expression: HK2 protein (J) and HK2 mRNA levels (K) in PC3 cells transfected with control vector, miR-143 expression vector or miR-143 mimic were determined by Western blot or RT-PCR. (L) Schematic model addressing HK2 upregulation upon p53 deletion. For Western blots, tubulin was used as a loading control. *P < 0.01. ns: not statistically significant.

Author Manuscript

Author Manuscript

Author Manuscript

Author Manuscript

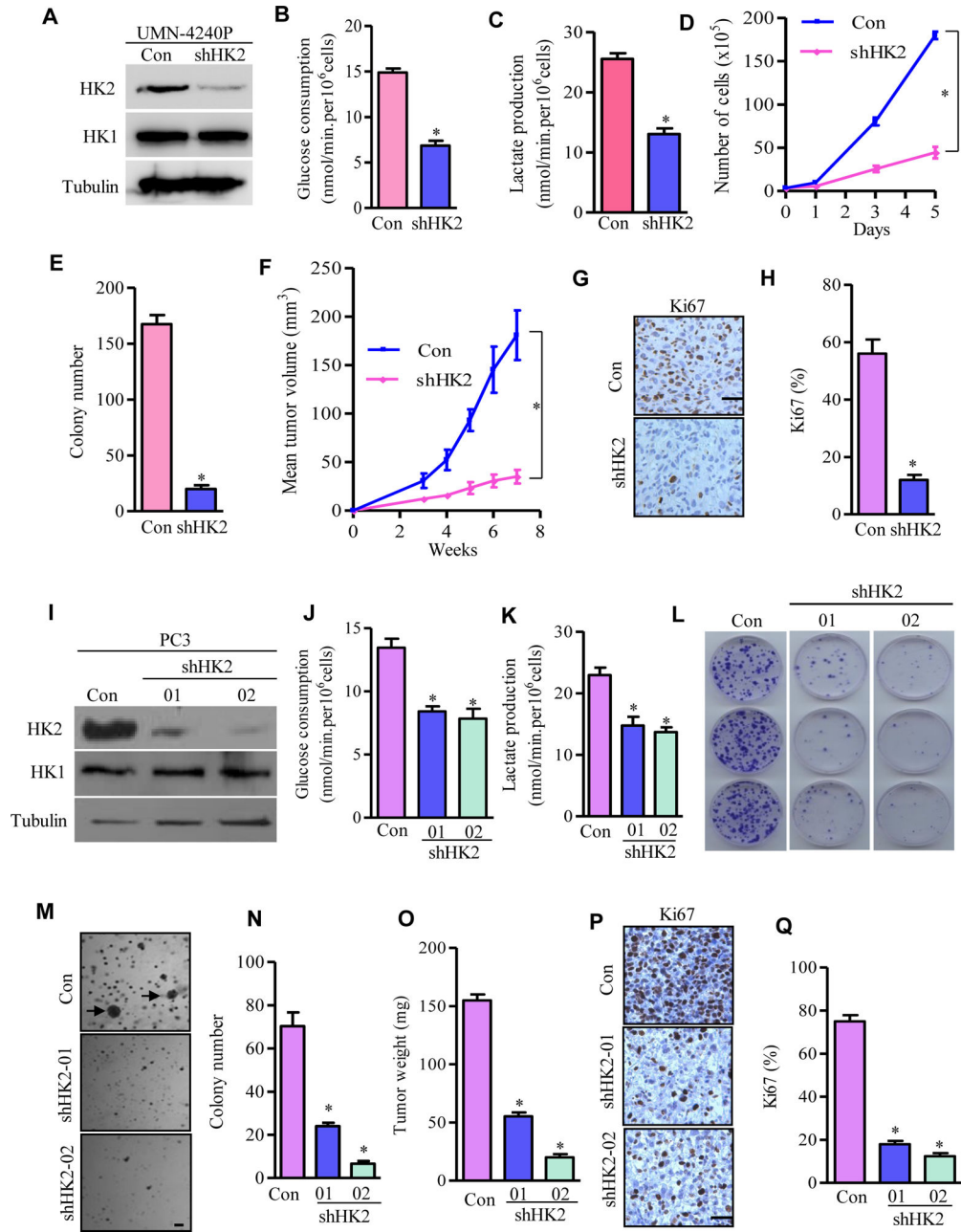


Figure 6. Depletion of HK2 Suppresses *Pten/p53*-Deficiency Driven Prostate Cancer Growth *in vivo*

(A–C) Knockdown of HK2 inhibits glycolysis in mouse prostate cancer cells. UMN-4240P prostate cancer cell line was transduced with scramble shRNA (Con) or shRNA targeting HK2 (shHK2). HK2 protein expression was detected by Western blotting (A). Glucose consumption (B) and lactate production (C) from control or HK2-depleted cells were analyzed. (D) Cell proliferation upon HK2 depletion in UMN-4240P cells. (E) Quantification of colonies generated by either control or HK2 knockdown UMN-4240P cells from three independent experiments. (F–H) HK2 depletion in UMN-4240P cells on prostate tumorigenesis *in vivo*. Tumor growth curve in xenografts carrying control or HK2-depleted

mouse prostate cancer cells (F), IHC staining of cell proliferation marker Ki67 (G), and its quantification (H) from G. (I–K) HK2 depletion inhibits glycolysis in human prostate cancer cells. PC3 cells were transfected with scramble shRNA (Con) or two independent shRNAs for HK2 (shHK2-01 and shHK2-02). HK2 was detected by Western blotting (I), Glucose consumption (J) and lactate production (K) from control or HK2-depleted PC3 cells were analyzed. (L) Colonies were stained by crystal violet after 10 days of cell growth. (M and N) Cell growth in soft agar and colonies were photographed and counted after 21 days. Representative images of colonies are shown and arrows indicate survival clones (M), and the bar graph shows the average number of colonies (\pm SEM) of triplicates (N). (O–Q) Xenograft tumor growth assay *in vivo*. Average tumor weight (O), IHC staining of cell proliferation marker Ki67 (P), and its quantification (Q) from tumors developed in NSG mice carrying control or HK2-depleted PC3 cells. All data are shown as means \pm S.E.M. For Western blots, tubulin was used as a loading control. *P \leq 0.01. Scale bar: 100 μ m.

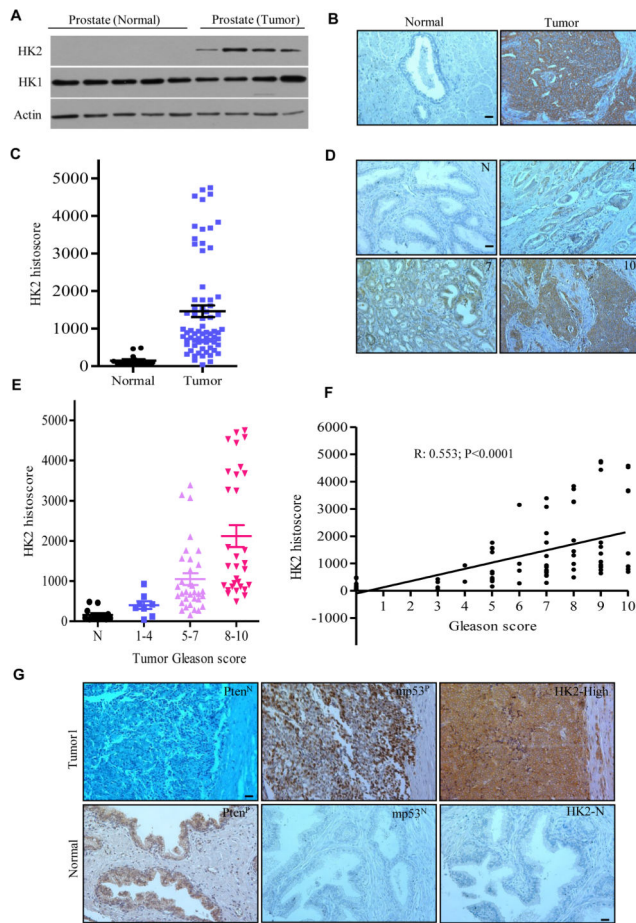


Figure 7. HK2 Is Elevated in Human Prostate Cancers

(A) Lysates from human normal prostate and prostate tumor was immunoblotted by the indicated antibodies. (B) IHC staining of HK2 expression in human normal prostate (n=15) and prostate tumors (n=70). Representative images of HK2 staining were shown. (C) Quantification of HK2 staining intensity was analyzed with Image-Pro plus (v 6.3) and shown in scatter plot. (D) IHC staining of HK2 expression in human normal prostate and prostate tumors with the indicated Gleason score. Representative images of HK2 staining in normal tissue and tumors with identified Gleason score were shown. (E) Quantification of HK2 staining intensity was analyzed with Image-Pro plus (v 6.3) and shown in scatter plot with Gleason score. TMA samples analyzed are as follows: 15 normal, 7 Gleason 1–4, 33 Gleason 5–7, and 30 Gleason 8–10. (F) Correlation between HK2 protein expression levels and Gleason score of human prostate cancer. Spearman's ρ was used to assess correlation. (G) Representative images of HK2 protein expression in human prostate cancer samples with negative Pten (Pten^N) and positive mutant p53 (mp53^P) were shown. Normal prostate tissue served as a positive control for Pten (Pten^P), negative controls for mutant p53 (mp53^N) and HK2 (HK2-N). Scale bar: 100 μ m. See also Figure S7.